Experimental Brain Research (2019) 237:573–583
https://doi.org/10.1007/s00221-018-5439-4

RESEARCH ARTICLE

Alterations in oscillatory cortical activity indicate changes in mnemonic processing during continuous item recognition

Sebastian Graetz[1] · Jonathan Daume[2] · Uwe Friese[1] · Thomas Gruber[1]

Received: 18 July 2018 / Accepted: 18 November 2018 / Published online: 28 November 2018

Abstract

The classification of repeating stimuli as either old or new is a general mechanism of everyday perception. However, the cortical mechanisms underlying this process are not fully understood. In general, mnemonic processes are thought to rely on changes in oscillatory brain activity across several frequencies as well as their interaction. Lower frequencies, mainly theta-band (3–7 Hz) and alpha-band (8–14 Hz) activity, are attributed to executive control and resource management, respectively; whereas recent studies revealed higher frequencies, e.g. gamma-band (> 25 Hz) activity, to reflect the activation of cortical object representations. Furthermore, low-frequency phase to high-frequency amplitude coupling (PAC) was recently found to coordinate the involved mnemonic networks. To further unravel the processes behind memorization of repeatedly presented stimuli, we applied a continuous item recognition task with up to five presentations per item (mean time between repetitions ~ 10 s) while recording high-density EEG. We examined spectral amplitude modulations as well as PAC. We observed theta amplitudes reaching a peak at second presentation, a reduction of alpha suppression after second presentation, decreased response time, as well as reduced theta–gamma PAC (3 to 7 to − 30 to 45 Hz) at frontal sites after third presentation. We conclude a shift from an explicit- to an implicit-like mnemonic processing, occurring around third presentation, with theta power to signify encoding of repetition-based episodic information and PAC as a neural correlate of the coordination of local neural networks.

Keywords EEG · Working memory · Oscillations · Cross-frequency coupling

Introduction

Mnemonic processes in the human brain are related to oscillatory brain activity in mainly three frequency bands in the theta, alpha and gamma range (Roux and Uhlhaas 2014). In a complex manner, oscillations within each band correlate with specific cognitive functions (Hanslmayr and Staudigl 2014).

Theta-band activity commonly refers to oscillations between approximately 3 and 7 Hz. In humans, these are most prominent in the hippocampus and in prefrontal areas (Headley and Paré 2017; Sirota et al. 2008). Theta-band activity is widely believed to reflect central executive functions, it is linked to successful encoding in declarative memory tasks (e.g. Klimesch et al. 2000; Heusser et al. 2016; Osipova et al. 2006; Roux and Uhlhaas 2014; Sederberg et al. 2003), retrieval (e.g. Jacobs et al. 2006; Osipova et al. 2006) and provides intermediate- and long-range connectivity between different brain areas (Sarnthein et al. 1998; Sauseng et al. 2004, 2005, 2010; for review see).

Alpha-band activity, neural oscillation in the frequency of approximately 8–14 Hz usually found at parieto-occipital recording sites, is assumed to mirror functional inhibition in visual memory tasks (e.g. Gevins et al. 1997; Jokisch and Jensen 2007; Klimesch et al. 2007). Task-relevant information, i.e. information that has to be attended, leads to decreased alpha activity in associated areas, whereas task-irrelevant information, i.e. information that has to be ignored, leads to increased alpha activity in associated areas (Hanslmayr and Staudigl 2014; Jensen and Mazaheri 2010; for review see Roux and Uhlhaas 2014).

✉ Sebastian Graetz
sebastian.graetz@uni-osnabrueck.de

1 Experimental Psychology I, Institute of Psychology, Osnabrück University, Neuer Graben 29, 49074 Osnabrück, Germany

2 Department of Neurophysiology and Pathophysiology, University Medical Center Hamburg-Eppendorf, Martinistraße 52, 20246 Hamburg, Germany

Neural gamma oscillations are a phenomenon which can be found in most cortical areas (Fries et al. 2007). Gamma-band activity, which encompasses oscillations upwards of approximately 25 Hz, in memory tasks is connected to successful encoding and retrieval (e.g. Gruber et al. 2004; Hanslmayr et al. 2008; Osipova et al. 2006) as well as feature integration (for a review see Jensen et al. 2007; Jutras and Buffalo 2010; Nyhus and Curran 2010). Gamma-band activity might therefore signify the activation of cortical object representations in a bottom-up or top-down fashion as shown in the seminal work by Tallon-Baudry and Bertrand (1999) and many other studies (e.g. Chaumon et al. 2009; Vidal et al. 2006). Importantly, mnemonic processing is not only dependent on oscillatory activity in a specific band, but the dynamic interplay of these oscillations (Lisman and Jensen 2013). This interaction is commonly referred to as cross-frequency coupling (CFC; for a schematic overview of different types of cross-frequency coupling, see Jensen and Colgin 2007). Various studies suggest that the most promising candidate mechanism for efficient mnemonic processing is the coupling of lower frequency phase information to higher frequency amplitudes (phase–amplitude coupling; PAC). PAC might be a core mechanism of neuronal communication in and across neural areas (e.g. Axmacher et al. 2010; Canolty et al. 2006; Canolty and Knight 2010; Friese et al. 2013; Köster et al. 2014). More specifically, PAC might be a prime candidate reflecting the regulating influence of frontal/executive brain areas on currently activated cortical representations of an item (Daume et al. 2017).

In a nutshell, theta oscillatory activity possibly marks the executive control over an activated memory representation, whereas gamma oscillatory activity signifies the activation itself. Alpha-band modulations might mirror the gating of attended or ignored information, respectively. The activity in specific frequency bands is coordinated by PAC. Noteworthy, from a conceptual perspective, an activated and situationally relevant representation in memory can be termed "working memory" (Ruchkin et al. 2003). This mechanistic view on mnemonic functioning is well in line with cognitive-psychological memory models, which focus on the function of the human storage system. One prominent example is the embedded-process model by Nelson Cowan (1999) also defining "working memory" as activated long-term memory traces within or outside a mental focus of attention (Cowan 2008). These claims are underpinned by EEG and MEG studies (e.g. Daume et al. 2017a, b; LaRocque et al. 2013; Lewis-Peacock et al. 2012). However, most of these studies examined the activation of memory traces by means of single-item presentations: a stimulus is presented once and it has to be matched to a sample after a delay period. These single-presentation designs do not completely reflect mnemonic processing as used in everyday life. Usually, we encounter items several times in short order and decide continuously if a stimulus is old or new. Thus, to examine oscillatory correlates in these situations, we applied a continuous item recognition task, similar to an fMRI design used by Johnson, Muftuler and Rugg (2008): in this paradigm, items are presented several times at random intervals. Each item has to be continuously classified as either old or new while recording high-density EEG.

Because of the general lack of prior EEG studies examining oscillatory neuronal activity with comparable designs, in the present study, we opted for an exploratory approach and omitted specific hypotheses regarding impact of repetition on oscillatory activity. Nonetheless, we expect theta and gamma oscillatory activity to increase with activation of relevant memory traces, accompanied by raised PAC over involved areas. Alpha oscillatory activity should be suppressed over task-relevant sites and increased over task-irrelevant sites.

Method

Participants

In accordance with numerous prior EEG studies twenty-two participants were recruited for the experiment. Two participants had to be excluded from further analyses: one because of low performance resulting in too few trials, i.e. eight, and thus a suboptimal signal-to-noise ratio; one because of extremely unusual motor responses. The remaining 20 were university students (M_{age} 22.4 years, SD 3.4 years) who received course credits for their participation. Unexpectedly, all remaining participants were female. No relevant health conditions or deviations from normal vision were reported by the participants. They each gave prior informed consent in accordance to the Declaration of Helsinki and the ethical guidelines of Osnabrück University. The present study was reviewed and approved by the local ethics committee of Osnabrück University.

Apparatus and stimuli

All instructions and stimulus material were presented on a 19 inch monitor (resolution: 1024 × 768 px, refresh rate: 60 Hz) while participant sat in an electrical and sound-shielded room. The stimulation software was coded in MATLAB (MathWorks) and the PsychToolbox (Brainard and Vision 1997; Kleiner et al. 2007).

The stimulus material consisted of 440 full-colour images showing natural objects (e.g. pumpkin, sunflower), man-made objects (e.g. screwdriver, golf ball), animals (e.g. cat, frog) and people in different attire (e.g. ballet dancer, bride). Pictures of all categories were randomly assigned to the conditions. They were presented centrally on the screen at a visual angle of approximately 4° × 4° from edge to edge (see Fig. 1 for examples).

Each participant performed a continuous item-recognition task while the EEG was recorded (see below). This task consisted of 702 trials separated into three blocks of equal length. The experiment was preceded by two practice blocks of four trials each. A trial started with a fixation cross (approx. 0.36° × 0.36°) for 500–1000 ms. Subsequently, a picture was presented for 1500 ms while participants had to classify the picture as fast as possible via button press into one of two categories: initial (NEW) vs. repeated (OLD). A picture could be shown once, twice or five times in total and at least 45 unique images were used in each condition (see Fig. 1a). After the picture, a fixation cross was presented for 800 ms during which participants were allowed to blink, if necessary. Repeatedly presented images were intervened by one up to six different pictures (time between repeated pictures: from approximately 3 to 18 s). Conditions for the later analysis were picture presentation count (one, two, three, four and five), i.e. the number of times the stimulus has been presented. As pictures could be shown once, twice or five times in total, the counts three, four and five include the same pictures. To ensure proper encoding of the presented items, an unannounced long-term old/new recognition task was administered after 24 h. Only trials which were correctly identified as being presented at day 1 were included in further analysis (on average ~ 15% percent of the trials had to be rejected).

EEG recordings

The EEG data were recorded with a BioSemi ActiveTwo system with 128 electrodes at 512 Hz sample rate during the task. Four electro-occulogram (EOG) electrodes were mounted at the outer canthi and below each eye to monitor for saccades and blinks. As ground and reference two additional electrodes were used, Common Mode Sense (CMS) and Driven Right Leg (DRL). The continuous data were epochized from − 1000 to 2000 ms relative to stimulus onset. Artefacts related to blinks, eye movements, muscle activity, and heart beat were removed by means of the FASTER toolbox (Nolan et al. 2010). Furthermore, we applied the COSTRAP algorithm (Hassler et al. 2011) to remove high-frequency artefacts attributed to miniature saccades. COSTRAP and similar ICA-based algorithms have been shown to effectively diminish these artefacts (Craddock et al. 2016) and were successfully applied in prior publications (e.g. Friese et al. 2013; Köster et al. 2014). The average reference was used for all further analyses. To guarantee for similar signal-to-noise ratios in all conditions, the remaining trials were matched in number across conditions (average number of trials per condition: 35, SD 8.7).

Design

This study was a three-level within-subject picture-based working memory experiment with picture presentation count (one, two, three, four, five) as independent variable. The dependent variables were response time, accuracy and electrophysiological markers; i.e. theta band, alpha band,

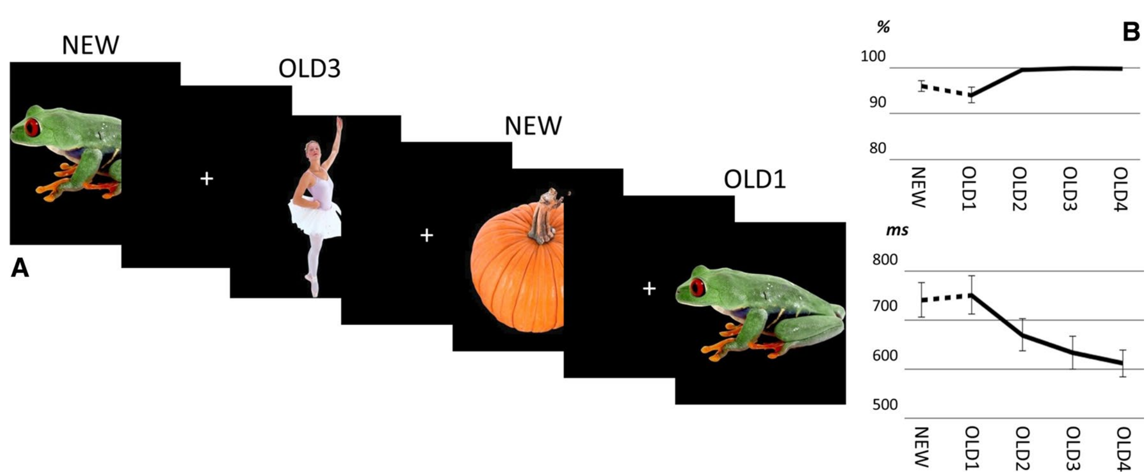

Fig. 1 **a** Stimulus/trial example. First-time presented pictures are marked as NEW. Repeated pictures are marked as OLD with a number indicating number of repetition; in the example given the ballet dancer has been repeated three times and the frog is repeated for the first time. **b** Lineplot of average accuracy in percentage (%) and reaction time in milliseconds (ms) for each repetition condition with error bars representing 95% confidence interval. For accuracy at OLD2, OLD3 and OLD4 95% confidence intervals are smaller than the line width

gamma-band activity and cross-frequency phase–amplitude coupling between theta and gamma-band activity.

Data analysis

The data analysis was conducted similar to previous studies (e.g. Gruber et al. 2008; Köster et al. 2014): we calculated the spectral changes in the oscillatory activity by means of Morlet's wavelet transform (Bertrand and Pantev 1994) using approximately 12 cycles per wavelet for the convolution with the data. We calculated the wavelets for frequencies from 2 to 100 Hz in approximately 1 Hz steps. To examine induced oscillatory activity we subtracted the ERP from each trial, computed the time-dependent spectral changes for each trial, and then averaged across trials (Bertrand and Tallon-Baudry 2000).

As we aimed to investigate changes in already established frequency ranges, we selected the following frequencies for further analyses: 4–7 Hz for theta activity, 9–13 Hz for alpha activity and 50–100 Hz for gamma activity. All selected frequencies are in line with prior research (e.g. Chaumon et al. 2009; Roux and Uhlhaas 2014).

Time × Frequency plots (TF-plots) of the grand mean were used to define relevant frequency time windows for further analyses. The TF-plots for lower frequencies, i.e. 3–20 Hz, and higher frequencies, i.e. 30–100 Hz, were averaged across all electrodes excluding those on the outer edge of the electrode setup (see Fig. 2a) and were baseline-corrected with baseline from − 500 to − 100 ms relative to stimulus onset. To outrule artefacts through temporal smearing, a minimum of 100 ms distance to stimulus onset was adhered to. Visual inspection of the corresponding TF-plots led to the selection of the following time windows: 100–700 ms for theta band, 200–1200 ms for alpha band and 100–700 ms for gamma-band activity in the range of 50–100 Hz (see Fig. 2a). All areas of interest were selected based on prior research (e.g. Chaumon et al. 2009; Roux and Uhlhaas 2014) and fitted to the specific grand mean topography for each time × frequency (see Fig. 2b). These topographical plots were created within EEGLAB (Delorme and Makeig 2004). Importantly, to avoid any bias regarding the selection of time and frequency ranges, we examined an average across all conditions for TF-plots as well as topographies in both, spectral power analyses and PAC.

Behaviour

The conditions for final analysis were first (NEW), second (OLD1), third (OLD2), fourth (OLD3) and fifth presentation (OLD4). A one-factorial repeated measurement ANOVA with five levels (REPETITION: NEW, OLD1, OLD2, OLD3, OLD4) was calculated and post-hoc *t* tests, with Bonferroni-corrected alpha-niveau of 0.005, followed were appropriate. Because of the emerging pattern, we also

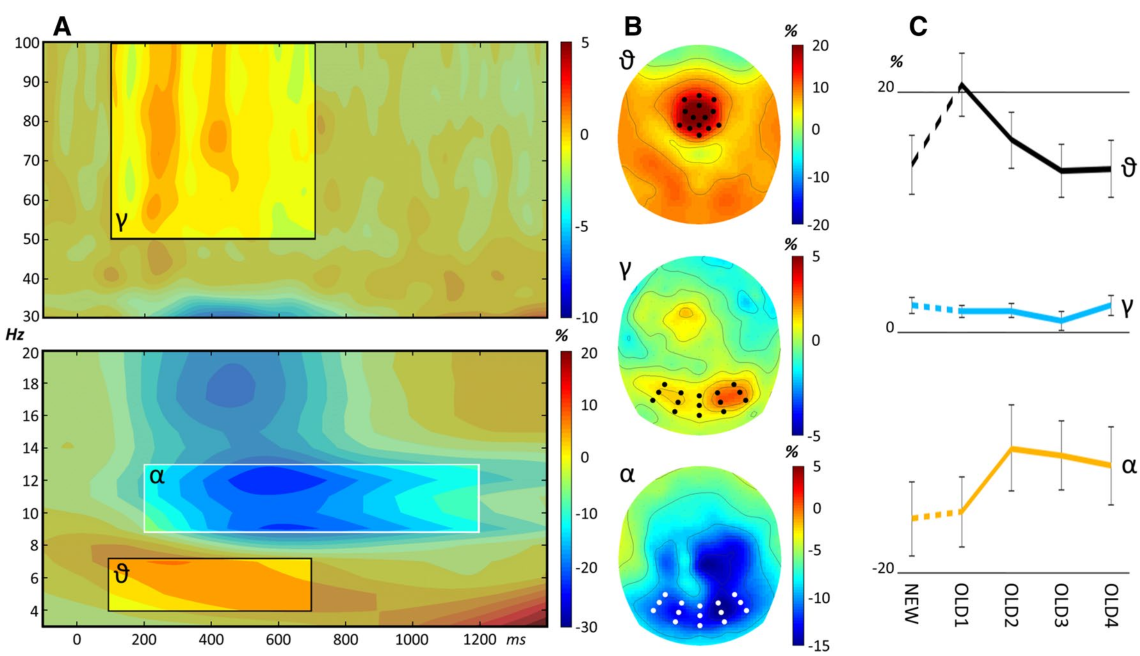

Fig. 2 **a** Time × frequency plots over whole scalp without cap rim electrodes. − 100 to 1400 ms relative to stimulus onset. 3–20 Hz lower and 30–100 Hz upper frequency ranges. Percentage change to baseline. Marked are time × frequency windows for topographies. **b** Topographies of marked time × frequency windows. Marked are electrodes for further statistical analysis. Percentage change to baseline. **c** Lineplot of average activity at electrode sites for each repetition condition. Percentage change to baseline. Error bars indicate SEM

calculated post-hoc *t* test between the mean across NEW and OLD1 versus the mean across remaining repetitions OLD2, OLD3 and OLD4.

Spectral power

Spectral power was analysed similar to the behavioural data: a one-factorial repeated measurement ANOVA with five levels (REPETITION: NEW, OLD1, OLD2, OLD3, OLD4) was calculated and post-hoc *t* tests, with Bonferroni-corrected alpha-niveau of 0.005, followed where appropriate. Because of the emerging alpha activity pattern, post-hoc *t* test between the mean across NEW and OLD1 and the mean across remaining repetitions OLD2, OLD3 and OLD4 were calculated, parallel to behavioural analysis. Also, to validate our results, we examined ERPs, namely the FN400 component (420 ms to 450 mx) and the LPC (470–500 ms) at conventional electrodes, i.e. F3 for FN400 and P3 for LPC (Rugg and Curran 2007).

Phase–amplitude coupling (PAC)

We quantified the phase–amplitude coupling by calculating the Modulation Index (MI; Tort et al. 2010). To determine the MI, one extracts the phase information from a lower frequency band and the amplitude from a higher frequency band. The phase angle of a full cycle is then divided into several bins, i.e., 20, so one bin represents 18°, and the average amplitude of the higher frequency is calculated for each bin. If no coupling is present, the distribution of the amplitude mean values should be approximately uniform across bins. In case of phase–amplitude coupling, a distribution different from uniform emerges. The divergence of this peak-distribution from an equal distribution is calculated by the Kullback–Leibler distance, modified to limit the result from 0 to 1 (Tort et al. 2010). Similar to Friese and colleagues (2013) we deviated from the suggested Hilbert transforms (Tort et al. 2010), by applying wavelet-analysis to extract phase and amplitude information, as the same wavelet transform was used in the spectral power analysis (for the legibility of this approach also see Kramer et al. 2008; Mormann et al. 2005). As the MI is influenced by data length (Tort et al. 2010), in that longer epochs allow a more reliable calculation of MI, we reshaped the trial data by concatenating trials into one continuous data stream (see also Daume et al. 2017). Trials were offset-corrected via an addition of the difference of the last data point of the prior trial and the starting point of the current trial to reduce influence of ripples, created by the sharp edge between two data points on different levels (Kramer et al. 2008). To reduce edge artefacts, we padded the concatenated trial data with half a second of mirrored data points at both ends prior to the wavelet transform. This padding was then removed afterwards.

For selecting possible theta–gamma interactions, we first calculated MI between the phase of frequencies from 3 to 9 Hz, to include the whole theta activity range, in 1 Hz steps and the amplitude for frequencies from 25 to 105 Hz, to include the whole gamma activity range, in steps of 5 Hz with a frequency window of 10 Hz around each target frequency, e.g. 45 Hz target frequency leads to 35–55 Hz window used as amplitude for the MI calculation. This calculation was done separately for each subject, condition and electrode. The time range was based on the theta time window of the spectral analyses, i.e. 100–700 ms after stimulus onset. As baseline we calculated the MI. In the same way, but for a time range from − 700 to − 100 ms relative to stimulus onset. To further narrow down frequency regions of interest, we created a comodulogram by averaging across subjects, conditions and electrodes, followed by dividing by each corresponding point of the baseline comodulogram. Visual inspection of the emerging comodulogram led to the selection of the coupling range for the subsequent analyses, i.e. 3–7 Hz phase to 30–45 Hz amplitude (see Fig. 3a). Furthermore, a grand mean topographical plot, showing the mean MI for each scalp electrode (Fig. 3b), was created based on this phase/amplitude frequency selection.

Based on this MI topography, we identified two appropriate regional means for statistical evaluations, namely a frontal and an occipital region (see Fig. 3a). For these regions, we calculated the MI for each condition, participant and frequency band separately; then averaged across relevant frequencies and participants and subtracted the equivalent baseline data. We conducted a two-factorial repeated measurement ANOVA with the factors SITE (2 levels: FRONTAL, OCCIPITAL) and REPETITION (5 levels: NEW, OLD1, OLD2, OLD3, OLD4), followed by post-hoc *t* tests.

In all ANOVAs the degrees of freedom were Greenhouse–Geisser corrected, if necessary. Effect strength measures used are partial η^2 for ANOVA and Cohen's *d* for *t* tests.

Results

Behavioural data

The repeated measurement ANOVA showed a main effect in response time (RT) for REPETITION [$F(2.356, 44.772) = 89.036$, $p < .001$, partial $\eta^2 = 0.824$; see Fig. 1b]. Participants response times did not differ for the first two presentations, NEW versus OLD1 [$t(19) = -0.798$, $p = .44$]. They became faster with each subsequent repetition [$t(19) > 3$, all $p < .005$, all $d > 0.29$]. Post-hoc *t* test between the mean RT across NEW and OLD1 versus the mean RT across OLD2, OLD3 and OLD4 revealed a large decrease in RT [$t(19) = 14.485$, $p < .001$, $d = 1.35$] after the first two presentations.

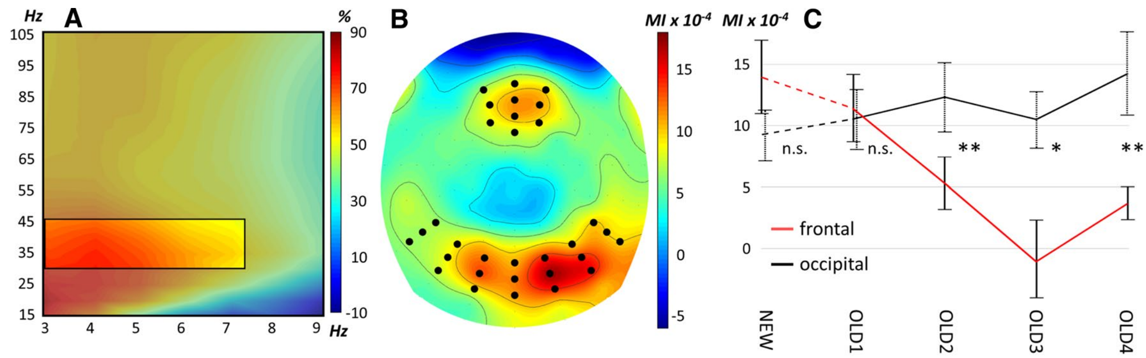

Fig. 3 **a** Comodulogram. Phase frequency 3–9 Hz, amplitude frequency 15–105 Hz in 5 Hz steps with a 10 Hz window centered around target frequency. Percentage change to baseline. Marked are phase × amplitude frequency window for topography. **b** Topographies of marked phase × amplitude frequency window. Marked are electrodes for further statistical analysis. **c** Lineplot of baseline corrected average MI for each repetition condition, error bars represent SEM. Significance of differences between locations for each condition is marked to the right side of each pair. $^{*}p < .05$; $^{**}p < .01$

The repeated measurement ANOVA also revealed a main effect in accuracy (ACC) for REPETITION [$F(1.987, 37.750) = 35.088$, $p < .001$, partial $\eta^2 = 0.649$; see Fig. 1b]. Similar to RT, the ACC at first two presentations did not differ [$t(19) = 2.502$, $p = .022$]. Participants became more accurate in their response over increasing repetition count, but hit a ceiling at OLD2, which did not differ from OLD3 and OLD4 [for comparisons between OLD2, OLD3 and OLD4, all $t(19) < 1$, $p > .3$; all remaining $t(19) > 5$, $p < .001$, $d < -2.0$]. Post-hoc t test between the mean ACC across NEW and OLD1 versus the mean ACC across OLD2, OLD3 and OLD4 revealed a large increase of accuracy after first two presentations [$t(19) = -8.093$, $p < .001$, $d = -1.35$].

RT and ACC are positively correlated up to OLD2 (NEW: $r = .31$, $p = .19$; OLD1: $r = .46$, $p = .04$; OLD2: $r = .50$, $p = .03$) and show a non-significant negative correlation for OLD3 and OLD4 (OLD3: $r = -.27$, $p = .26$; OLD4: $r = -.17$, $p = .47$). Averaging across conditions revealed a medium effect strength confound between RT and ACC ($r = .46$, $p = .04$).

ERPs (FN400 and LPC)

We found the FN400 at 420–450 ms and the LPC at 470–500 ms (see Fig. 4). The FN400 was reduced with each subsequent presentation [$F(2.525, 47.982) = 4.661$, $p = .009$, partial $\eta^2 = 0.197$]. The LPC was increased for each subsequent presentation [$F(2.448, 46.509) = 6.879$, $p = .001$, partial $\eta^2 = 0.266$]. We observed no meaningful correlation between ERP amplitudes and our oscillatory measures (Bonferroni corrected $p = .01$; all $p > .02$).

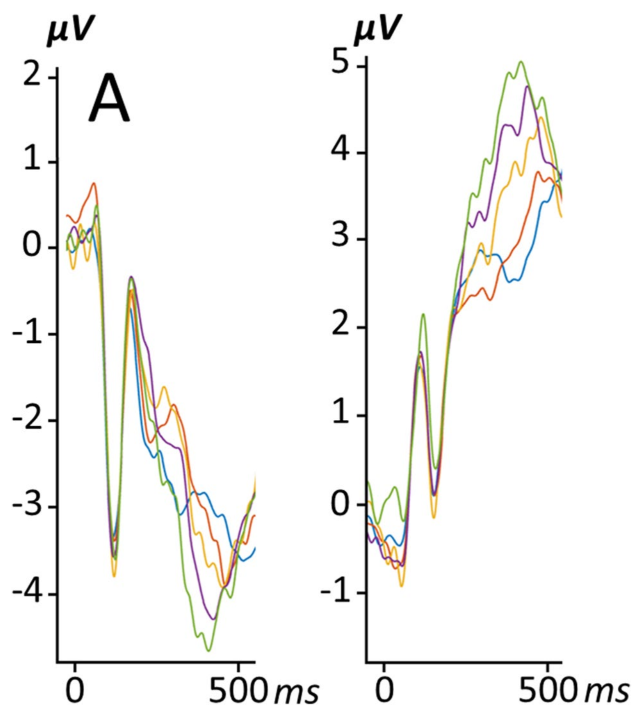

Fig. 4 **a** ERPs averaged across signals at electrodes in the vicinity of sensor F3. **b** ERPs averaged across signals at electrodes in the vicinity of sensor P3. Each line represents one condition: NEW (blue), OLD1 (red), OLD2 (yellow), OLD3 (violet), OLD4 (green)

Spectral changes

Time by frequency plots revealed stimulus-triggered increase of activity between 100 and 700 ms after stimulus onset in theta band (4–7 Hz; Fig. 2a). A decrease of alpha-band activity emerged around 200–1200 ms (9–13 Hz; Fig. 2a). As well as an increase in gamma-band activity (50–100 Hz) between 100 and 700 ms (Fig. 2a).

Topographical distributions revealed typical local maxima for each frequency band, i.e. medio-frontal sites for theta, parieto-occipital sites for alpha and occipital electrodes for gamma activity. Further statistical analyses were conducted with data obtained from these electrode sites (Fig. 2b).

Fronto-medial theta-band activity changed with REPETITION [$F(4, 76) = 10.036$, $p < .001$, partial $\eta^2 = 0.346$; see Fig. 2c]. Theta-band activity peaked at OLD1, differing from all other conditions [$t(19) > 3.4$, $p < .005$, $d > 0.7$]. The remaining conditions did not differ from each other (all $p > .005$).

Alpha-band activity at parieto-occipital electrodes revealed less suppression as the number of repetitions increased [$F(4, 76) = 3.065$, $p = .021$, partial $\eta^2 = 0.139$; see Fig. 2c]. Post-hoc t test showed only one significant difference between NEW and OLD3 [$t(19) = -3.182$, $p < .005$, $d = 0.7$; all remaining $p > .005$]. But post-hoc t test between the mean activity across NEW and OLD1 versus the mean across OLD2, OLD3 and OLD4 revealed that overall alpha-band activity increased after the first two repetitions [$t(19) = -3.674$, $p = .002$, $d = -0.37$]. Interestingly, this reduction of alpha suppression, which is normally associated with lowering task demand, mirrors the pattern of the improvement of both behavioural outcomes.

Gamma-band activity revealed no main effect for REPETITION at occipital sites [$F(4, 76) = 1.141$, $p = .344$; see Fig. 2c]. Note: as some spectral changes appeared to lateralize, namely alpha-band activity, gamma-band activity and the posterior coupling measures (see Figs. 2, 3), we calculated additional ANOVA with hemisphere as a factor. No relevant interactions were significant.

Theta gamma phase–amplitude coupling (PAC)

The repeated Measurement two-factorial ANOVA revealed no significant modulation of the MI by SITE [$F(1,19) = 3.516$, $p = .076$, partial $\eta^2 = 0.156$], but a main effect for CONDITION [$F(4, 76) = 2.886$, $p = .028$, partial $\eta^2 = 0.132$], which is further characterized by the interaction between SITE and CONDITION [$F(2.333, 44.331) = 8.060$, $p = .001$, partial $\eta^2 = 0.298$]. During the first two presentations, the MI did not differ between frontal and occipital sites [NEW: $t(19) = 1.374$, $p = .185$; OLD1: $t(19) = 0.319$, $p = .753$]. All remaining presentations resulted in a lower MI over frontal sites [OLD2: $t(19) = -2.954$, $p = .008$, $d = -0.68$; OLD3: $t(19) = -2.701$, $p = .014$, $d = -0.61$; OLD4: $t(19) = -2.930$, $p = .009$, $d = -0.72$; see Fig. 3c]. Interestingly, the reduction in frontal MI also mirrors the pattern of alpha power and the behavioural outcome measures, with the first two presentations resulting in a more pronounced MI than the remaining presentations [$t(19) = 3.636$, $p = .002$, $d = 1.02$]. No such effect was found for the occipital MI [$t(19) = -1.179$, $p = .25$].

To rule out possible influences of theta power fluctuation on the MI, we calculated correlations between theta power at relevant coupling sites and the MI. We found one significant result at frontal sites for OLD3 ($r = .49$, $p = .028$, all other $p > .2$, all r between $r = -.28$ and $r = -.02$) and two correlations at occipital sites for OLD3 and OLD4 (OLD3: $r = -.435$, $p = .055$; OLD4: $r = -.449$, $p = .047$; all other $p > .4$, all other r between $r = -.17$ and $r = .07$). If theta power were systematically influencing MI calculation, we would expect at least medium strength correlations in the same direction between theta power and MI for all conditions. As this is clearly not the case, we consider these results as spurious correlations.

Discussion

In the present EEG study, we applied a continuous item recognition task, to investigate oscillatory brain activity as well as cross-frequency coupling during the repeated (re-) activation of memory entries. Although the participants were unexpectedly all female, we do not consider this fact to influence our results in an interpretable fashion.

The behavioural data, i.e. response times and accuracy, are in accordance with prior results in similar tasks (e.g. Johnson et al. 2008). As would be expected, repetition lead to better performance (Yonelinas 2002; Yassa and Stark 2008). Thus, the experimental design was well suited to measure mnemonic performance during the repetition of task-relevant objects. In particular, accuracy and response time are consistent for first and second presentation. For further repetitions, accuracy increases, reaching a ceiling at third presentation, whereas participants also became faster in responding to learned items. Accuracy and response time were clearly confounded overall, but an accurate interpretation of this confound is limited by the ceiling of accuracy. Therefore, we focus on response times in our discussion. Interestingly, a sharp alteration from the second to the third presentation is obvious in both behavioural measures. This alteration might indicate a change in the underlying mnemonic processes. The continuous decrease in reaction times from the second repetition onwards might indicate a priming-like phenomenon, i.e. the facilitation in the processing of previously presented stimuli (*cf.* Tulving and Schacter 1990). Speculatively, our behavioural data suggest that the participants automatically switched from an explicit- to an implicit-like mnemonic processing after the second presentation of an object. In other words, the first recognition of an item as “old” might be related to a resource-intensive process (explicit), whereas repeated presentations could be recognized by a resource-tolerant (implicit) process (Graf and Schacter 1985). This alteration of mnemonic processing is accompanied by specific electrophysiological indices, which we will discuss in detail in the following section.

We found increased theta-band activity at fronto-medial recording sites. This topographical localisation replicates the result of prior working memory research (for review, see Roux and Uhlhaas 2014). As expected, theta amplitude was elevated during all conditions. However, it showed a marked increase after the second presentation of a stimulus and decreases to the initial response level for further repetitions. This decrease after second presentation mirrors response time data. The general increase in theta power matches prior results (Sauseng et al. 2010; Sederberg et al. 2006) and supports the notion of increased executive function demands during mnemonic processing, i.e. executive control over activated memory (Cowan 1999). The maximum increase of theta after the second presentation is in line with previous observations reporting a similar pattern of results after the second presentation of meaningful objects after repetition (Gruber and Müller 2006). These authors speculated that the theta increase during the repeated item presentation is related to recollection-related mechanisms (Gruber and Müller 2006), i.e. the encoding and retrieval of additional episodic information related to the repeated stimulus (Curran 1999). Interestingly, in our study, the theta amplitude decreases back to the level of the initial presentation in response to the third, fourth, and fifth appearance. Thus, it is unlikely to be a general correlate of repeated presentation. If one assumes that theta is related to recollection-related processes, it has to be concluded that further repetitions do not trigger the encoding and retrieval of additional episodic information. Speculatively, the processing of the stimuli presented for a third time (or more often) might be accompanied by familiarity related mnemonic mechanisms, i.e. the automatic experience that a stimulus was observed before (for similar interpretations see, e.g. Burgess and Ali 2002; Gruber and Müller 2006). It is important to note, even though our paradigm was not specifically designed to explore familiarity and recollection, as postulated in the dual process theory (Wixted 2007), the results so far point towards such a model. This explanation, a facilitation of processing by reducing the amount of encoded and retrieved information, is underpinned by our reaction time data.

In line with our hypothesis, alpha activity was generally suppressed over occipital and parietal areas, as has been also reported in several prior visual task studies (e.g. Jokisch and Jensen 2007; Klimesch et al. 2007; for review see; Roux and Uhlhaas 2014). More specifically, we found a pattern similar to our behavioural results, i.e. a sharp alteration of alpha amplitudes from the second to the third presentation. The larger alpha suppression over left-parieto and occipital sites during the first two presentations might indicate a disinhibition of task-relevant areas (Roux and Uhlhaas 2014), since the task up to second presentation was relatively demanding. Starting with third presentation, we observed an increase in performance accompanied by a less pronounced alpha suppression.

This is in line with our proposed switching from explicit to implicit retrieval processing: as more features of an item are encoded and/or retrieved from memory during explicit retrieval, more neuronal areas/resources need to be involved, requiring reduced alpha suppression. During implicit retrieval, the process is a less resource intensive task, resulting in a relative lack of alpha suppression. One could of course argue, that repetition merely leads to a practice effect, i.e. a reduction of required resources with each repetition. The pattern we observed, relatively strong suppression for first two presentations followed by a strong one-time lessening of the suppression for the following presentations, stands in contrast to that notion: obviously, a practice effect should reveal a linear pattern, without any marked non-monotonous changes in the dependent variables. This does not exclude effects of task practice on the observed data.

As predicted, we observed an overall increase of gamma-band activity over posterior sites, as has been reported in various studies (e.g. Hassler et al. 2013; Friese et al. 2012a, b). This posterior gamma-band activity seems to mirror the activation of a cortical object representation driven by visual perceptive input (Chaumon et al. 2009, Tallon-Baudry and Betrand 1999; Vidal et al. 2006). Interestingly, gamma amplitudes did not vary with item repetition. Thus, one might speculate that a similar cortical representation of an object is activated with each presentation. This stands in contrast to previous research claiming that item repetition is accompanied by repetition suppression, i.e. a reduction of neuronal responses elicited by repeated items (Wiggs and Martin 1998; Friese et al. 2012). One explanation for this phenomenon is the assumption that with each repetition less features of an object representation need to be activated to meet task demands. However, repetition suppression is primarily observed when the repetition of an item is task-irrelevant and the processing of the repeated item is solely based on implicit mechanisms (cf. Gruber and Müller 2006). Based on the interpretation proposed above, i.e. from the third presentation onwards, our task might be solved by means of implicit mnemonic processes, one has to conclude that gamma suppression is not the sole neuronal correlate of this mechanism and a more complex interplay of processes is involved.

A likely candidate for the neural correlate of this complex interplay is phase–amplitude coupling (PAC). PAC was found to be elevated at mid-frontal and at occipital sites. These topographical distributions are in line with prior research (e.g. Canolty et al. 2006 for frontal; Canolty and Knight 2010; Friese et al. 2013; Heusser et al. 2016 for occipital). As the changes in PAC show a different pattern for frontal compared to occipital sites, they possibly fulfill different task-specific functions related to visual working memory (Canolty et al. 2006). This also fits the notion, that visual working memory in general is closely associated with activity in the prefrontal and posterior cortex (Xu 2017). In our study PAC at occipital sites was found to be elevated and insensitive to item repetition. This finding might mirror a general mechanism of associative visual processing: when an object is presented, corresponding information is retrieved from prior established memory, signified by gamma activity and maintained via ongoing theta activity. This proposed process matches activated long-term memory, as defined in the embedded process model (Cowan 1999). In contrast, PAC at frontal sites shows a similar pattern to alpha activity and the behavioural results, i.e. a sharp alteration from second to third presentation. As PAC diminishes with third and ongoing presentation, the underlying processes seem to be unnecessary or, as PAC is still slightly elevated, at least demanded less to fulfil the task requirement during the third, fourth and fifth presentation of a stimulus. Most likely, this PAC represents coordination of frontal executive or mnemonic networks relevant in explicit mnemonic processing, i.e. active matching of memory content with active perception content. After the second presentation, the need for this frontal executive network is diminished, as the task can be successfully solved with less resource-intensive processes. This result, of two different PAC patterns at different locations during one task, is further evidence, that PAC is a general neural process used for "transient coordination of local networks on short time scales" (Jensen and Colgin 2007).

The FN400 and the LPC ERP components, i.e. conventional markers of mnemonic processing, do not sufficiently mirror the complex interplay of cognitive function evident in the present experimental design. Both components were modulated in a linear fashion with the number of presentations. The interpretation of these results based on the literature is difficult, since in our design the filler items between two task-relevant repetitions were task-relevant as well. In our opinion, the most likely explanation is a simple repetition effect revealed in the ERPs.

Several other factors might have influenced our behavioural and electrophysiological measures, namely performance anxiety and reduction of task novelty. Increased performance anxiety would most likely result in reduction of performance measurements (Johnson and Gronlund 2009), whereas reduction of task novelty, i.e. practice, most likely has positive effects on these measurements (Yonelinas 2002). Both variables might influence brain oscillations. As we have neither assessed performance anxiety nor reduction of task novelty directly, we cannot assume these to affect every participant (or experiment block) equally. However, the expected direction of these influences goes in opposite direction reducing the likelihood of a systemic bias.

In conclusion, continuous item repetition, similar to the real-world experience of stimuli, requires the coordination of several underlying mnemonic processes. We observed changes in theta and alpha-band activity, as well as coupling measures over frontal areas to mirror changes in response time over repeated presentations. This study was a first step in illuminating possible characteristics of memory mechanisms during multiple item repetition. We propose, a change from explicit-like to implicit-like mnemonic retrieval processes underlying the observed alterations in numerous oscillatory markers of brain activity: frontal theta-band activity could reflect general executive functions accompanying explicit and implicit retrieval processes; posterior alpha-band activity marks disinhibition of neural areas involved in attention towards memory traces. Posterior gamma-band activity signifies the activation of neuronal object representation. The coordinative and communicative demands of the involved neural networks during continuous memory are managed via phase–amplitude cross-frequency coupling in theta–gamma range.

Acknowledgements This work was supported by grants from the German Research Foundation (GR2684/5-1). We thank Moritz Köster for helpful methodological discussions, and Simeon Platte, Sophia Sylvester and Marlene Wessels for assistance in data recording.

Funding This work was supported by grants from the German Research Foundation (GR2684/5-1).

Compliance with ethical standards

Conflict of interest The authors declare that they have no conflict of interest.

Ethical approval All procedures performed in studies involving human participants were in accordance with the ethical standards of the Osnabrück University and with the 1964 Helsinki Declaration and its later amendments or comparable ethical standards. This study was reviewed and approved by the local ethics committee of Osnabrück University.

Informed consent Informed consent was obtained from all individual participants included in the study.

References

Axmacher N, Henseler MM, Jensen O, Weinreich I, Elger CE, Fell J (2010) Cross-frequency coupling supports multi-item working memory in the human hippocampus. Proc Natl Acad Sci 107(7):3228–3233

Bertrand O, Pantev C (1994) Stimulus frequency dependence of the transient oscillatory auditory evoked responses (40 Hz) studied by electric and magnetic recordings in human. In: Oscillatory event-related brain dynamics. Springer US, New York, pp 231–242

Bertrand O, Tallon-Baudry C (2000) Oscillatory gamma activity in humans: a possible role for object representation. Int J Psychophysiol 38(3):211–223

Brainard DH, Vision S (1997) The psychophysics toolbox. Spat Vis 10:433–436

Burgess AP, Ali L (2002) Functional connectivity of gamma EEG activity is modulated at low frequency during conscious recollection. Int J Psychophysiol 46(2):91–100

Canolty RT, Knight RT (2010) The functional role of cross-frequency coupling. Trends Cogn Sci 14(11):506–515

Canolty RT, Edwards E, Dalal SS, Soltani M, Nagarajan SS, Kirsch HE, Berger MS, Barbaro NM, Knight RT (2006) High gamma power is phase-locked to theta oscillations in human neocortex. Science 313(5793):1626–1628

Chaumon M, Schwartz D, Tallon-Baudry C (2009) Unconscious learning versus visual perception: dissociable roles for gamma oscillations revealed in MEG. J Cogn Neurosci 21(12):2287–2299

Cowan N (1999) An embedded-processes model of working memory. Models of working memory. Mech Active Maint Exec Control 20:506

Cowan N (2008) What are the differences between long-term, short-term, and working memory? Progress Brain Res 169:323–338

Craddock M, Martinovic J, Müller MM (2016) Accounting for microsaccadic artifacts in the EEG using independent component analysis and beamforming. Psychophysiology 53(4):553–565

Curran T (1999) The electrophysiology of incidental and intentional retrieval: erp old/ new effects in lexical decision and recognition memory. Neuropsychologia 37(7):771–785

Daume J, Graetz S, Gruber T, Engel AK, Friese U (2017a) Cognitive control during audiovisual working memory engages frontotemporal theta-band interactions. Sci Rep 7(1):12585

Daume J, Gruber T, Engel AK, Friese U (2017b) Phase-amplitude coupling and long-range phase synchronization reveal frontotemporal interactions during visual working memory. J Neurosci 37(2):313–322

Delorme A, Makeig S (2004) EEGLAB: an open source toolbox for analysis of single-trial EEG dynamics including independent component analysis. J Neurosci Methods 134(1):9–21

Fries P, Nikolić D, Singer W (2007) The gamma cycle. Trends Neurosci 30(7):309–316

Friese U, Supp GG, Hipp JF, Engel AK, Gruber T (2012a) Oscillatory MEG gamma band activity dissociates perceptual and conceptual aspects of visual object processing: a combined repetition/conceptual priming study. Neuroimage 59(1):861–871

Friese U, Rahm B, Hassler U, Kaiser J, Gruber T (2012b) Repetition suppression and effects of familiarity on blood oxygenation level dependent signal and gamma-band activity. Neuroreport 23(13):757–761

Friese U, Köster M, Hassler U, Martens U, Trujillo-Barreto N, Gruber T (2013) Successful memory encoding is associated with increased cross-frequency coupling between frontal theta and posterior gamma oscillations in human scalp-recorded EEG. Neuroimage 66:642–647

Gevins A, Smith ME, McEvoy L, Yu D (1997) High-resolution EEG mapping of cortical activation related to working memory: effects of task difficulty, type of processing, and practice. Cereb Cortex (New York, NY: 1991) 7(4):374–385

Graf P, Schacter DL (1985) Implicit and explicit memory for new associations in normal andamnesic subjects. J Exp Psychol Learn Mem Cogn 11(3):501

Gruber T, Müller MM (2006) Oscillatory brain activity in the human EEG during indirect and direct memory tasks. Brain Res 1097(1):194–204

Gruber T, Tsivilis D, Montaldi D, Müller MM (2004) Induced gamma band responses: an early marker of memory encoding and retrieval. Neuroreport 15(11):1837–1841

Gruber T, Tsivilis D, Giabbiconi CM, Müller MM (2008) Induced electroencephalogram oscillations during source memory: familiarity is reflected in the gamma band, recollection in the theta band. J Cogn Neurosci 20(6):1043–1053

Hanslmayr S, Staudigl T (2014) How brain oscillations form memories—a processing based perspective on oscillatory subsequent memory effects. Neuroimage 85:648–655

Hanslmayr S, Spitzer B, Bäuml KH (2008) Brain oscillations dissociate between semantic and nonsemantic encoding of episodic memories. Cereb Cortex 19(7):1631–1640

Hassler U, Trujillo-Barreto N, Gruber T (2011) Induced gamma band responses in human EEG after the control of miniature saccadic artifacts. Neuroimage 57(4):1411–1421

Hassler U, Friese U, Martens U, Trujillo-Barreto N, Gruber T (2013) Repetition priming effects dissociate between miniature eye movements and induced gamma-band responses in the human electroencephalogram. Eur J Neurosci 38(3):2425–2433

Headley DB, Paré D (2017) Common oscillatory mechanisms across multiple memory systems. npj Sci Learn 2(1):1

Heusser AC, Poeppel D, Ezzyat Y, Davachi L (2016) Episodic sequence memory is supported by a theta–gamma phase code. Nat Neurosci 19(10):1374

Jacobs J, Hwang G, Curran T, Kahana MJ (2006) EEG oscillations and recognition memory: theta correlates of memory retrieval and decision making. Neuroimage 32(2):978–987

Jensen O, Colgin LL (2007) Cross-frequency coupling between neuronal oscillations. Trends Cogn Sci 11(7):267–269

Jensen O, Mazaheri A (2010) Shaping functional architecture by oscillatory alpha activity: gating by inhibition. Front Hum Neurosci 4:186

Jensen O, Kaiser J, Lachaux JP (2007) Human gamma-frequency oscillations associated with attention and memory. Trends Neurosci 30(7):317–324

Johnson DR, Gronlund SD (2009) Individuals lower in working memory capacity are particularly vulnerable to anxiety's disruptive effect on performance. Anxiety Stress Coping 22(2):201–213

Johnson JD, Muftuler LT, Rugg MD (2008) Multiple repetitions reveal functionally and anatomically distinct patterns of hippocampal activity during continuous recognition memory. Hippocampus 18(10):975–980

Jokisch D, Jensen O (2007) Modulation of gamma and alpha activity during a working memory task engaging the dorsal or ventral stream. J Neurosci 27(12):3244–3251

Jutras MJ, Buffalo EA (2010) Synchronous neural activity and memory formation. Curr Opin Neurobiol 20(2):150–155

Kleiner M, Brainard D, Pelli D, Ingling A, Murray R, Broussard C (2007) What's new in Psychtoolbox-3. Perception 36(14):1

Klimesch W, Doppelmayr M, Schwaiger J, Winkler T, Gruber W (2000) Theta oscillations and the ERP old/new effect: independent phenomena? Clin Neurophysiol 111(5):781–793

Klimesch W, Sauseng P, Hanslmayr S (2007) EEG alpha oscillations: the inhibition-timing hypothesis. Brain Res Rev 53(1):63–88

Köster M, Friese U, Schöne B, Trujillo-Barreto N, Gruber T (2014) Theta–gamma coupling during episodic retrieval in the human EEG. Brain Res 1577:57–68

Kramer MA, Tort AB, Kopell NJ (2008) Sharp edge artifacts and spurious coupling in EEG frequency comodulation measures. J Neurosci Methods 170(2):352–357

LaRocque JJ, Lewis-Peacock JA, Drysdale AT, Oberauer K, Postle BR (2013) Decoding attended information in short-term memory: an EEG study. J Cogn Neurosci 25(1):127–142

Lewis-Peacock JA, Drysdale AT, Oberauer K, Postle BR (2012) Neural evidence for a distinction between short-term memory and the focus of attention. J Cogn Neurosci 24(1):61–79

Lisman JE, Jensen O (2013) The theta-gamma neural code. Neuron 77(6):1002–1016

Mormann F, Fell J, Axmacher N, Weber B, Lehnertz K, Elger CE, Fernández G (2005) Phase/amplitude reset and theta–gamma

interaction in the human medial temporal lobe during a continuous word recognition memory task. Hippocampus 15(7):890–900
Nolan H, Whelan R, Reilly RB (2010) FASTER: fully automated statistical thresholding for EEG artifact rejection. J Neurosci Methods 192(1):152–162
Nyhus E, Curran T (2010) Functional role of gamma and theta oscillations in episodic memory. Neurosci Biobehav Rev 34(7):1023–1035
Osipova D, Takashima A, Oostenveld R, Fernández G, Maris E, Jensen O (2006) Theta and gamma oscillations predict encoding and retrieval of declarative memory. J Neurosci 26(28):7523–7531
Roux F, Uhlhaas PJ (2014) Working memory and neural oscillations: alpha–gamma versus theta–gamma codes for distinct WM information? Trends Cogn Sci 18(1):16–25
Ruchkin DS, Grafman J, Cameron K, Berndt RS (2003) Working memory retention systems: a state of activated long-term memory. Behav Brain Sci 26(6):709–728
Rugg MD, Curran T (2007) Event-related potentials and recognition memory. Trends Cogn Sci 11(6):251–257
Sarnthein J, Petsche H, Rappelsberger P, Shaw GL, Von Stein A (1998) Synchronization between prefrontal and posterior association cortex during human working memory. Proc Natl Acad Sci 95(12):7092–7096
Sauseng P, Klimesch W, Doppelmayr M, Hanslmayr S, Schabus M, Gruber WR (2004) Theta coupling in the human electroencephalogram during a working memory task. Neurosci Lett 354(2):123–126
Sauseng P, Klimesch W, Schabus M, Doppelmayr M (2005) Fronto-parietal EEG coherence in theta and upper alpha reflect central executive functions of working memory. Int J Psychophysiol 57(2):97–103
Sauseng P, Griesmayr B, Freunberger R, Klimesch W (2010) Control mechanisms in working memory: a possible function of EEG theta oscillations. Neurosci Biobehav Rev 34(7):1015–1022
Sederberg PB, Kahana MJ, Howard MW, Donner EJ, Madsen JR (2003) Theta and gamma oscillations during encoding predict subsequent recall. J Neurosci 23(34):10809–10814
Sederberg PB, Gauthier LV, Terushkin V, Miller JF, Barnathan JA, Kahana MJ (2006) Oscillatory correlates of the primacy effect in episodic memory. NeuroImage 32(3):1422–1431
Sirota A, Montgomery S, Fujisawa S, Isomura Y, Zugaro M, Buzsáki G (2008) Entrainment of neocortical neurons and gamma oscillations by the hippocampal theta rhythm. Neuron 60(4):683–697
Tallon-Baudry C, Bertrand O (1999) Oscillatory gamma activity in humans and its role in object representation. Trends Cogn Sci 3(4):151–162
Tort AB, Komorowski R, Eichenbaum H, Kopell N (2010) Measuring phase-amplitude coupling between neuronal oscillations of different frequencies. J Neurophysiol 104(2):1195–1210
Tulving E, Schacter DL (1990) Priming and human memory systems. Science 247(4940):301–306
Vidal JR, Chaumon M, O'Regan JK, Tallon-Baudry C (2006) Visual grouping and the focusing of attention induce gamma-band oscillations at different frequencies in human magnetoencephalogram signals. J Cogn Neurosci 18(11):1850–1862
Wiggs CL, Martin A (1998) Properties and mechanisms of perceptual priming. Curr Opin Neurobiol 8(2):227–233
Wixted JT (2007) Dual-process theory and signal-detection theory of recognition memory. Psychol Rev 114(1):152
Xu Y (2017) Reevaluating the sensory account of visual working memory storage. Trends Cogn Sci 21(10):794–815
Yassa MA, Stark CE (2008) Multiple signals of recognition memory in the medial temporal lobe. Hippocampus 18(9):945–954
Yonelinas AP (2002) The nature of recollection and familiarity: a review of 30 years of research. J Mem Lang 46(3):441–517